Optimal Evasion Against Dual Pure Pursuit*

Alexander Von Moll[1], Zachariah Fuchs[2], and Meir Pachter[3]

***Abstract*— The Pure Pursuit strategy is ubiquitous both in the control literature but also in real-world implementation. In this paper, we pose and solve a variant of Isaacs' Two Cutters and Fugitive Ship problem wherein the Pursuers' strategy is fixed to Pure Pursuit, thus making it an optimal control problem. The Pursuers are faster than the Evader and are endowed with a finite capture radius. All agents move with constant velocity and can change heading instantaneously. Although capture is inevitable, the Evader wishes to delay capture as long as possible. The optimal trajectories cover the entire state space. Regions corresponding to either solo capture or isochronous (dual) capture are computed and both types of maximal time-to-capture optimal trajectories are characterized.**

I. Introduction

The scenario of pursuit and evasion is one that is rooted in the natural interactions of predator and prey and has applications to modern warfare. In this paper we consider optimal evasion against two faster Pursuers who employ a Pure Pursuit (PP) strategy – that is, the Pursuers' instantaneous headings are always along their respective line-of-sight (LOS) to the Evader's position. The Evader wishes to extend its life as long as possible before being captured by the Pursuers. All three agents move with *simple motion*, i.e., with constant velocity and no heading rate constraint. Capture occurs when either one, or both, Pursuers come within range d_c of the Evader.

This scenario is a variation on the classical Two Cutters and Fugitive Ship differential game originally posed by Isaacs [1]. In the Two Cutters and Fugitive Ship differential game, the Pursuers, acting as a team, wish to capture the Evader in the shortest time possible, while the Evader, as in this case, wishes to delay capture, thus making it a zero-sum differential game. Isaacs' treatment of the problem was geometrical, based on the fact that all three agents' saddle point equilibrium strategies result in straight-line paths [1]. Additionally, Isaacs was focused on point capture, except in the case of the closely related game of capture on a wall. Isaacs rightfully noted that point capture in two or more dimensions yields a degenerate terminal surface and demonstrated how a proper terminal surface (e.g., when one endows the Pursuer(s) with a finite capture radius, d_c) alleviates issues like the *perpetual dilemma* [1]. The geometric solution to the game was then validated in [2] by expressing the Value function associated with the geometric solution analytically and showing that it satisfies the Hamilton-Jacobi-Isaacs equation. Reference [3] sought to show the applicability of the two-pursuer one-evader solution to scenarios with more than two pursuers. In [4], the solution to the Game of Kind (i.e., whether capture by the first, or second, or both Pursuers simultaneously) is given using a reduced state space. The consequences of the Dispersal Surface in the game were considered in [5]. The case of a finite capture radius was then considered in [6], [7]. In the former, the solution is based on a system of two nonlinear equations obtained by analytic retrograde integration of the optimal dynamics; this solution also covers the case of Pursuers with different speeds. The latter provides a closed-form solution for the case where all three agents have the same speed.

The biggest difference in this paper compared with the aforementioned works is the fact that, rather than playing the game, the Pursuers' strategy is fixed (to PP). Although differential game theory is considered to be a generalization of optimal control [1], it is sometimes the case that fixing the strategy of one of the sides can make the analysis more challenging. For example, the solution to the one-on-one pursuit-evasion differential game with simple motion, which is for the Evader to run directly from the Pursuer and for the Pursuer to run directly towards the Evader, is almost trivial to show using differential game analysis. However, if it is assumed that the Pursuer employs PP, the optimal control analysis (which yields the same optimal action for the Evader) is not trivial (c.f. [8]) due to the nonlinearity of the dynamics induced by the Pursuers' PP state-feedback strategy. This exercise of optimizing an agent's strategy against a particular opponent's strategy, even when the game scenario has been solved, is useful when that opponent strategy is so widely used or well-known, as is the case for PP. For example, in [8], a Target and Defender cooperate against an Attacker who employs PP. Similarly, [9], [10] consider the same scenario but with an Attacker who employs Proportional Navigation (PN) (with finite capture radius and point capture, respectively). The scenario described in this paper was also considered in [11] wherein it was assumed that the Pursuers employ either PP or a fixed heading strategy. There, in the PP case, point capture was considered and the optimal control problem was solved using numerical pseudo-spectral (collocated) methods. Here, we emphasize the analytical approach.

The obvious application for this scenario is an aerial

*The views expressed in this paper are those of the authors and do not reflect the official policy or position of the United States Air Force, Department of Defense, or the United States Government.

[1] Alexander Von Moll is with the Control Science Center of Excellence, Air Force Research Laboratory, WPAFB, OH 45433, USA alexander.von_moll@us.af.mil

[2] Zachariah Fuchs is with the Department of Electrical Engineering and Computer Science, University of Cincinnati, Cincinnati, OH 45221, USA fuchsze@mail.uc.edu

[3] Meir Pachter is with the Department of Electrical Engineering, Air Force Institute of Technology, WPAFB, OH 45433, USA meir.pachter@afit.edu

vehicle evading two incoming kinetic weapons (e.g. beyond visual range missiles). There is some merit to this as two missiles are regularly fired to increase the probability of kill (see, e.g. [12]). However, the main interest in considering this particular problem is to obtain a fundamental building block to be used in bigger engagement scenarios. In this respect, both [13] and [14] consider the game version of the multiple-pursuer one-evader problem. In [14] the solution to the two-pursuer one-evader game was used to construct a robust Pursuer policy for the case of multiple Pursuers. Reference [15] considers the multiple-pursuer, multiple-evader scenario with fixed Pursuer strategies by utilizing the results of sub-problems (e.g. two-on-one) in a task allocation framework (c.f. also, [16]).

The main contributions of this paper are (1) the synthesis of the optimal evasion control law against dual pure pursuit with finite capture radius, (2) characterization of the disjoint regions of the state space corresponding to the different capture cases, (3) proofs regarding the set of terminal Evader headings resulting in optimal dual capture, and (4) a backwards shooting numerical method for solving the Two-Point Boundary Value Problem (TPBVP) arising where indirect optimization is employed. The paper is organized as follows. Section II contains the optimal control problem formulation and Section III contains a derivation of the optimality conditions. Section IV characterizes the solutions for both solo and dual capture. Section VI concludes the paper with remarks on the utility of this solution and identifies future research directions.

II. Problem Formulation

Let $E = (x_E, y_E)$, $P_1 = (x_1, y_1)$, and $P_2 = (x_2, y_2)$ denote the Evader, Pursuer 1, and Pursuer 2 and their respective positions in the realistic plane $\mathbb{R}^2$. The agents' velocities are denoted v_E, and $v_1 = v_2 = v_P$, respectively, and $v_E < v_P$. In the realistic plane, the state $\mathbf{x}_G \in \mathbb{R}^6$ has six components corresponding to the coordinates of the three agents in the Euclidean plane. For the remainder of the paper, we utilize a relative state space $\mathbf{x} \in \mathbb{R}^6$ based on the Evader's instantaneous position. The angle β is the angle of the line EP_1 w.r.t. the realistic x-axis. In later optimality analysis, it will be shown that only the first three state components influence the optimal solution: the Euclidean distances between each Pursuer and the Evader, d_1 and d_2, and the half-angle between the Pursuers w.r.t the Evader, α. Fig. 1 shows these key state components (black) along with the remaining state components (blue) used to relate the relative state to the realistic (global) state. The following equations relate the relative state to the global state,

$$\begin{bmatrix} x_E \\ y_E \\ x_1 \\ y_1 \\ x_2 \\ y_2 \end{bmatrix} = \begin{bmatrix} x \\ y \\ x + d_1\cos(\beta) \\ y + d_1\sin(\beta) \\ x + d_2\cos(\beta + 2\alpha) \\ y + d_2\sin(\beta + 2\alpha) \end{bmatrix}. \tag{1}$$

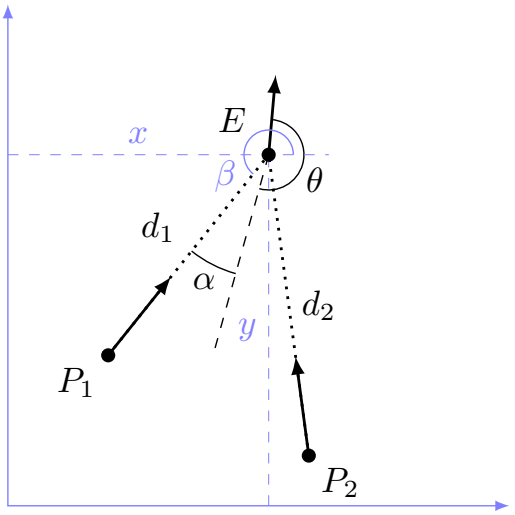

Fig. 1. Coordinate systems for the evasion scenario with main features and relative states in black and global states in blue.

The dimensional dynamics (denoted with a bar) are given as,

$$f = \begin{bmatrix} \dot{\bar{d}}_1 \\ \dot{\bar{d}}_2 \\ \dot{\bar{\alpha}} \\ \dot{\bar{x}} \\ \dot{\bar{y}} \\ \dot{\bar{\beta}} \end{bmatrix} = \begin{bmatrix} -v_E\cos(\theta + \bar{\alpha}) - v_P \\ -v_E\cos(\theta - \bar{\alpha}) - v_P \\ \frac{v_E}{2}\left(\frac{1}{\bar{d}_1}\sin(\theta + \bar{\alpha}) - \frac{1}{\bar{d}_2}\sin(\theta - \bar{\alpha})\right) \\ v_E\cos\left(\bar{\beta} + \bar{\alpha} + \theta\right) \\ v_E\sin\left(\bar{\beta} + \bar{\alpha} + \theta\right) \\ -\frac{v_E}{\bar{d}_1}\sin(\theta + \bar{\alpha}) \end{bmatrix}. \tag{2}$$

A. Non-Dimensionalization

Let the capture radius be denoted d_c, and the ratio of Evader to Pursuer speed be denoted $\mu = v_E/v_P < 1$. It is useful to consider the dimensionless form of the state $\mathbf{x}$ and its dynamics f because, in doing so, we effectively reduce the number of parameters from three (v_E, v_P, and d_c) to one (μ). Let non-dimensional distances be defined by $d = \bar{d}/d_c$ and non-dimensional time be defined by $t = \bar{t}/t_c$, where $t_c = d_c/v_P$ is the amount of time taken by a Pursuer to traverse the capture distance. Then the non-dimensional distance dynamics are obtained from

$$\begin{aligned} \dot{\bar{z}} = \frac{\mathrm{d}\bar{z}}{\mathrm{d}\bar{t}} = \frac{\mathrm{d}(d_c z)}{\mathrm{d}(t_c t)} = \frac{d_c}{t_c}\frac{\mathrm{d}z}{\mathrm{d}t} = \frac{d_c}{t_c}\dot{z} \\ \implies \dot{z} = \frac{t_c}{d_c}\dot{\bar{z}} = \frac{1}{v_P}\dot{\bar{z}}, \end{aligned} \tag{3}$$

for $z = d_1, d_2, x, y$ and the non-dimensional angular dynamics are obtained from

$$\begin{aligned} \dot{\bar{\psi}} = \frac{\mathrm{d}\bar{\psi}}{\mathrm{d}\bar{t}} = \frac{\mathrm{d}\psi}{\mathrm{d}(t_c t)} = \frac{1}{t_c}\frac{\mathrm{d}\psi}{\mathrm{d}t} = \frac{1}{t_c}\dot{\psi} \\ \implies \dot{\psi} = t_c\dot{\bar{\psi}} = \frac{d_c}{v_P}\dot{\bar{\psi}}, \end{aligned} \tag{4}$$

for $\psi = \alpha, \beta$. Substituting Eqs. (3) and (4) into Eq. (2) yields the non-dimensional form of the dynamics,

$$f = \begin{bmatrix} \dot{d}_1 \\ \dot{d}_2 \\ \dot{\alpha} \\ \dot{x} \\ \dot{y} \\ \dot{\beta} \end{bmatrix} = \begin{bmatrix} -\mu\cos(\theta+\alpha) - 1 \\ -\mu\cos(\theta-\alpha) - 1 \\ \frac{\mu}{2}\left(\frac{1}{d_1}\sin(\theta+\alpha) - \frac{1}{d_2}\sin(\theta-\alpha)\right) \\ \mu\cos(\beta+\alpha+\theta) \\ \mu\sin(\beta+\alpha+\theta) \\ -\frac{\mu}{d_1}\sin(\theta+\alpha) \end{bmatrix}. \quad (5)$$

B. Problem Statement

The problem for the Evader is to select its heading control $\theta(t)$, $t \in [0, t_f]$ to maximize the time to capture. The cost functional is,

$$J = \int_0^{t_f} (-1)\,\mathrm{d}t = \int_0^{t_f} L\,\mathrm{d}t = -t_f. \quad (6)$$

Note that, due to the non-dimensionalization, the scenario terminates (capture occurs) when either one or both Pursuers come within a non-dimensional distance of 1 to the Evader. The associated boundary condition is given as

$$\phi(\mathbf{x}_0, t_f, \mathbf{x}_f) = \left(d_{1_f} - 1\right)\left(d_{2_f} - 1\right) = 0, \quad (7)$$

where $\mathbf{x}_0$ and $\mathbf{x}_f$ are the initial and final states, respectively. We now express the optimal control problem as

$$\min_{\theta(t)} J, \text{ s.t. } \dot{\mathbf{x}} = f(\mathbf{x}, \theta), \ \phi = 0. \quad (8)$$

III. Optimality Conditions

The Hamiltonian is given by,

$$\begin{aligned}\mathscr{H} = {} & \lambda_{d_1}\left(-\mu\cos(\theta+\alpha) - 1\right) \\ & + \lambda_{d_2}\left(-\mu\cos(\theta-\alpha) - 1\right) \\ & + \lambda_\alpha \frac{\mu}{2}\left(\frac{1}{d_1}\sin(\theta+\alpha) - \frac{1}{d_2}\sin(\theta-\alpha)\right) \\ & + \lambda_x \mu\cos(\beta+\alpha+\theta) + \lambda_y \mu\sin(\beta+\alpha+\theta) \\ & - \lambda_\beta \frac{\mu}{d_1}\sin(\theta+\alpha) - 1 \end{aligned} \quad (9)$$

where $\lambda \equiv \begin{bmatrix}\lambda_{d_1} & \lambda_{d_2} & \lambda_\alpha & \lambda_x & \lambda_y & \lambda_\beta\end{bmatrix}^\top$ are the adjoint variables, the partial derivatives of the Value function. From the first order optimality conditions, the optimal adjoint dynamics are

$$\dot{\lambda}_{d_1} = -\frac{\partial\mathscr{H}}{\partial d_1} = \frac{\lambda_\alpha \mu\sin(\theta+\alpha)}{2d_1^2} \quad (10)$$

$$\dot{\lambda}_{d_2} = -\frac{\partial\mathscr{H}}{\partial d_2} = \frac{\lambda_\alpha \mu\sin(\theta-\alpha)}{2d_2^2} \quad (11)$$

$$\dot{\lambda}_\alpha = -\frac{\partial\mathscr{H}}{\partial\alpha} \quad (12)$$

$$\begin{aligned} & = -\lambda_{d_1}\mu\sin(\theta+\alpha) - \lambda_{d_2}\mu\sin(\theta-\alpha) \\ & \quad - \lambda_\alpha\frac{\mu}{2}\left(\frac{1}{d_1}\cos(\theta+\alpha) + \frac{1}{d_2}\cos(\theta-\alpha)\right) \end{aligned} \quad (13)$$

$$\dot{\lambda}_x = -\frac{\partial\mathscr{H}}{\partial x} = 0 \quad (14)$$

$$\dot{\lambda}_y = -\frac{\partial\mathscr{H}}{\partial y} = 0 \quad (15)$$

$$\dot{\lambda}_\beta = -\frac{\partial\mathscr{H}}{\partial\beta} = 0. \quad (16)$$

Because this is a free final time problem with a Lagrange cost functional, the transversality condition gives

$$\begin{aligned}\lambda^\top(t_f) &= \nu\frac{\partial\phi}{\partial\mathbf{x}_f} \\ &= \nu\begin{bmatrix}\left(d_{2_f} - 1\right) & \left(d_{1_f} - 1\right) & 0 & 0 & 0 & 0\end{bmatrix}\end{aligned} \quad (17)$$

$$\implies \lambda_{\alpha_f} = \lambda_{x_f} = \lambda_{y_f} = \lambda_{\beta_f} = 0. \quad (18)$$

Since the adjoint variables λ_x, λ_y, and λ_β are zero at final time (Eq. (18)) and their derivatives are zero (Eqs. (14)–(16)) they are zero for all time and thus the states x, y, and β have no effect on the optimality of the solution; only the d_1, d_2, and α states are pertinent. Substituting $\lambda_x = \lambda_y = \lambda_\beta = 0$ and using Ptolemy's Trigonometric Identities to expand the cosine/sine of sum terms in Eq. (9) yields,

$$\begin{aligned}\mathscr{H} = {} & -\lambda_{d_1}\mu\left(\cos\theta\cos\alpha - \sin\theta\sin\alpha\right) - \lambda_{d_1} - \\ & \lambda_{d_2}\mu\left(\cos\theta\cos\alpha + \sin\theta\sin\alpha\right) - \lambda_{d_2} + \\ & \lambda_\alpha\frac{\mu}{2}\left(\frac{1}{d_1}\left(\sin\theta\cos\alpha + \cos\theta\sin\alpha\right) - \right. \\ & \left. \frac{1}{d_2}\left(\sin\theta\cos\alpha - \cos\theta\sin\alpha\right)\right) - 1. \end{aligned} \quad (19)$$

Now define the following two quantities which are the coefficients of the $\cos\theta$ and $\sin\theta$ terms,

$$\begin{aligned}c_{\cos} = {} & \mu\left(-\lambda_{d_1}\cos\alpha - \lambda_{d_2}\cos\alpha + \frac{\lambda_\alpha}{2}\right. \\ & \left.\sin\alpha\left(\frac{1}{d_1} + \frac{1}{d_2}\right)\right) \end{aligned} \quad (20)$$

$$c_{\sin} = \mu\left(\lambda_{d_1}\sin\alpha - \lambda_{d_2}\sin\alpha + \frac{\lambda_\alpha}{2}\cos\alpha\left(\frac{1}{d_1} - \frac{1}{d_2}\right)\right) \quad (21)$$

and substitute back into (19) and simplify to get,

$$\mathscr{H} = c_{\cos}\cos\theta + c_{\sin}\sin\theta - \lambda_{d_1} - \lambda_{d_2} - 1. \quad (22)$$

From Pontryagin's Minimum Principle (PMP), then, the optimal heading is given by $\theta^* = \arg\min_\theta \mathscr{H}$. To minimize

$\mathscr{H}$, we must have the vector $\begin{bmatrix}\cos\theta & \sin\theta\end{bmatrix}^\top$ be antiparallel to the vector $\begin{bmatrix}c_{\cos} & c_{\sin}\end{bmatrix}$, giving,

$$\cos\theta^* = \frac{-c_{\cos}}{\sqrt{c_{\cos}^2 + c_{\sin}^2}},\ \sin\theta^* = \frac{-c_{\sin}}{\sqrt{c_{\cos}^2 + c_{\sin}^2}}. \tag{23}$$

The Hamiltonian at final time is given by,

$$\mathscr{H}(t_f) = -\nu\frac{\partial\phi}{\partial t_f} = 0. \tag{24}$$

Since $\mathscr{H}$ is not an explicit function of time, we have also that $\mathscr{H}(t) = 0,\ \forall t \in [0, t_f]$.

IV. Solution Characterization

We are interested in both solo and dual capture. Eq. (7) is satisfied for all three terminal scenarios: both the solo capture cases (i.e., $d_{1_f} > 1$ and $d_{2_f} = 1$, or vice versa) as well as the dual capture case ($d_{1_f} = d_{2_f} = 1$). We will develop optimal solutions for each of these cases in the following subsections.

A. Solo Capture

The first case is solo capture where $d_{1_f} = 1$ and $d_{2_f} > 1$, or $d_{1_f} > 1$ and $d_{2_f} = 1$.

Lemma 1 (Solo capture trajectories)**.** *The optimal control resulting in solo capture by P_1 is $\theta^*(t) = \pi - \alpha(t)$, $\forall t \in [0, t_f]$, and for solo capture by P_2 is $\theta^*(t) = \pi + \alpha(t)$, $\forall t \in [0, t_f]$.*

Proof. Consider the second case: solo capture by P_2, which entails $d_{2_f} = 1$ and $d_{1_f} > 1$. From Eq. (17), $\lambda_{d_{1_f}} = 0$, $\lambda_{d_{2_f}} = \nu\left(d_{1_f} - 1\right)$, and $\lambda_{\alpha_f} = 0$. Substituting these terminal adjoint values into Eqs. (20) and (21) gives,

$$c_{\cos} = -\mu\nu(d_{1_f} - 1)\cos\alpha_f,\ c_{\sin} = -\mu\nu(d_{1_f} - 1)\sin\alpha_f.$$

Substituting these values into the optimal control Eq. (23) gives,

$$\cos\theta_f^* = \operatorname{sign}(\nu)\cos\alpha_f,\ \sin\theta_f^* = \operatorname{sign}(\nu)\sin\alpha_f.$$

If $\operatorname{sign}(\nu) = 1$ then $\theta_f^* = \alpha_f$, which implies the E heads directly towards P_2, which is clearly suboptimal. Instead, if $\operatorname{sign}(\nu) = -1$ then $\theta_f^* = \pi + \alpha_f$, implying E heads directly away from P_2. Substituting this terminal Evader heading into the adjoint dynamics Eqs. (10)–(13) gives,

$$\dot\lambda_{d_{1_f}} = 0,\ \dot\lambda_{d_{2_f}} = 0,\ \dot\lambda_{\alpha_f} = 0,$$

which implies that the optimal adjoint values are constant over the trajectory. Then, from the above analysis, the condition $\theta^* = \pi + \alpha$ holds for all $t \in [0,\ t_f]$. By symmetry, the result $\theta^* = \pi - \alpha$ applies for solo capture by P_1. □

Lemma 2 (Solo capture trajectory shape)**.** *In the case of solo capture, the Evader's and capturing Pursuer's trajectories are straight lines in the realistic plane.*

Proof. Without loss of generality, consider solo capture by P_1. From Lemma 1 the Evader's optimal control is $\theta^*(t) = \pi - \alpha(t)$. The Evader's heading in the realistic plane is given by $\Theta = \beta + \alpha + \theta$. Substituting the optimal control in gives $\Theta = \beta + \pi$. The rate of change of the global Evader heading is $\dot\Theta = \dot\beta$. From Eq. (5) $\dot\beta \propto \sin(\theta + \alpha)$. Substituting the optimal control in makes $\dot\beta = 0$, thereby making $\dot\Theta = 0$. Thus the Evader's heading in the realistic plane is constant, implying a straight-line path. The Evader's heading lies along the line of sight $\overline{P_1E}$, and thus P_1's path is also straight. □

Remark. Note this is also the solution to the single-Pursuer single-Evader optimal control problem (c.f. [8]), and so the presence of the second Pursuer did not affect the optimal trajectories.

Lemma 3 (Closer Pursuer)**.** *Optimal solo capture is always executed by the Pursuer who began closer to the Evader.*

Proof. Without loss of generality, consider solo capture by P_1. From Lemma 1 the Evader's optimal control is $\theta^*(t) = \pi - \alpha(t)$. Therefore, from Eq. (5) and $\mu < 1$, we have $0 > \dot d_1(t) > \dot d_2(t)$, $\forall t \in [0, t_f]$. Since solo capture by P_1 entails $d_{1_f} = 1 < d_{2_f}$ it must be the case that $d_2(t) > d_1(t)$, $\forall t \in [0, t_f]$. □

There may be initial conditions for which optimal solo capture trajectories do not exist. For example, if E flees from whichever P is closer at initial time (following Lemmas 1 and 3) and ends up being captured by the other P, then optimal solo capture does not exist. It may also be the case that the optimal solo capture trajectory exists but an optimal dual capture trajectory exists.

Lemma 4. *If, for a particular initial condition, both solo capture and dual capture trajectories exist and satisfy all of the optimality conditions, the solo capture trajectory is uniquely optimal.*

Proof. From the definition of ϕ in (7) the dual capture candidate solution satisfies all of the optimality conditions for solo capture. However, Lemma 1 specifies the optimal control for solo capture ($\theta^* = \pi - \alpha$ for P_1 or $\theta^* = \pi + \alpha$ for P_2). Any other control action would result in a smaller t_f compared to the solo capture candidate solution. Therefore, the solo capture solution is optimal. □

B. Dual Capture

In the case of dual capture both $d_{1_f},\ d_{2_f} = 1$. However, if these terminal distances are substituted into Eq. (17) then $\lambda_{d_{1_f}} = \lambda_{d_{2_f}} = 0$. Substituting these values for the terminal distance adjoints (along with all of the other known terminal adjoints) gives $\mathscr{H}(t_f) = -1$ which contradicts Eq. (24), which says that $\mathscr{H}(t_f) = 0$. Dual capture, thus, exhibits a singularity, which is also evident by the fact that the terminal surface corresponding to dual capture, $\{d_1, d_2, \alpha \mid d_1 = d_2 = 1\}$, is a line $\in \mathbb{R}^1$. Isaacs states [1] that a non-degenerate terminal surface be of dimension one less than the dimension of the state space. The consequence, here, is that many different trajectories terminate at the same point on the dual capture termination line, even for the same terminal α. In order to proceed, we consider the limiting Evader heading, $\theta^*(t),\ t \to t_f$ and its relationship to the

limiting adjoint values using a procedure described in [6]:

$$\tan\theta^*(t_f) = \lim_{t\to t_f}\tan\theta^* = \lim_{t\to t_f}\frac{-c_{\sin}}{-c_{\cos}} = \lim_{t\to t_f}\frac{\sin\alpha_f\left(\lambda_{d_{2_f}}-\lambda_{d_{1_f}}\right)}{\cos\alpha_f\left(\lambda_{d_{2_f}}+\lambda_{d_{1_f}}\right)}.$$

Rearranging this expression for the adjoint variables yields

$$\kappa \equiv \frac{\lambda_{d_{2_f}}}{\lambda_{d_{1_f}}} = \frac{\tan\alpha_f + \tan\theta_f^*}{\tan\alpha_f - \tan\theta_f^*}. \tag{25}$$

Substituting the relation (25), along with (18) into Eqs. (9) and (24) and solving for the terminal distance adjoints yields,

$$\lambda_{d_{1_f}} = \frac{1}{-\mu\cos(\theta_f+\alpha_f) - 1 + \kappa\left(-\mu\cos(\theta_f-\alpha_f)-1\right)} \tag{26}$$

or,

$$\lambda_{d_{2_f}} = \frac{1}{\frac{1}{\kappa}\left(-\mu\cos(\theta_f+\alpha_f)-1\right) - \mu\cos(\theta_f-\alpha_f) - 1}. \tag{27}$$

Lemma 5. *At $\theta_f = \pi \pm \alpha$ the dual capture solution is equivalent to a solo capture solution with the non-capturing Pursuer's terminal distance approaching 1.*

Proof. From Eq. (25), we have $\kappa = 0$ when $\theta_f = \pi - \alpha$ and $\kappa = \infty$ when $\theta_f = \pi + \alpha$ which imply $\lambda_{d_{1_f}} \neq 0$ and $\lambda_{d_{2_f}} = 0$, or $\lambda_{d_{1_f}} = 0$ and $\lambda_{d_{2_f}} \neq 0$, respectively. Thus, when one of the terminal distance adjoints is zero and the other is non-zero, then from the analysis in Lemma 1 the optimal control is $\theta^*(t) = \pi \pm \alpha(t)$ over the whole trajectory. Therefore, the trajectories are identical to the solo capture case wherein the non-capturing Pursuer's terminal distance approaches 1. □

Proposition 1 (Optimal θ_f for dual capture)**.** *The range $\theta_f \in (\pi-\alpha, \pi+\alpha)$ produces globally optimal trajectories, and the trajectories produced by $\theta_f \notin (\pi-\alpha, \pi+\alpha)$ are suboptimal.*

Proof. From Eq. (25) whenever $\theta_f \notin [\pi-\alpha_f, \pi+\alpha_f]$ the terminal adjoint ratio $\kappa < 0$. This implies that the terminal distance adjoints, $\lambda_{d_{1_f}}$ and $\lambda_{d_{2_f}}$, have different signs; thus one of either $\lambda_{d_{1_f}} > 0$ or $\lambda_{d_{2_f}} > 0$. Suppose, without loss of generality that $\lambda_{d_{1_f}} > 0$. Equation (18) states that $\lambda_{\alpha_f} = 0$ – based on the optimal adjoint dynamics, Eq. (10), λ_{d_1} is not changing at final time. Thus $\lambda_{d_1} > 0$ for some nonzero time leading up to final time due to the smoothness of Eqs. (10)-(13). The adjoint variable $\lambda_{d_1} \equiv \frac{\partial V}{\partial d_1}$ where $V = \min_{\theta(t)} J$ is the Value function. Thus if $\lambda_{d_1} > 0$ the Value *increases* as distance from P_1 increases. Since the cost functional is the negative of final time, increasing the distance from P_1 is a disadvantage to the E, in this case. Contrariwise, when $\theta_f \in [\pi-\alpha_f, \pi+\alpha_f]$ for dual capture, and in the single capture case, $\lambda_{d_1}, \lambda_{d_2} \leq 0 \forall t$. Thus in the latter, optimal, cases, increasing distance from a Pursuer reduces the Value, which is advantageous for the E. In the absence of turning-rate constraints, increasing distance from a Pursuer (whilst keeping the other distance constant) should always benefit E. Consequently, dual capture with $\theta_f \notin [\pi-\alpha_f, \pi+\alpha_f]$ must be suboptimal. □

Remark. The terminal Evader headings $\theta_f \in (\alpha_f, \pi-\alpha_f) \cup (\pi+\alpha_f, 2\pi-\alpha_f)$, although suboptimal for this scenario (i.e., when both solo and dual capture are possible), are optimal for a scenario in which *only* dual capture is desired. Suppose E is defending some other target against the Pursuers and, after interception, is destroyed. In that scenario, the Evader wishes to collide with the two Pursuers simultaneously.

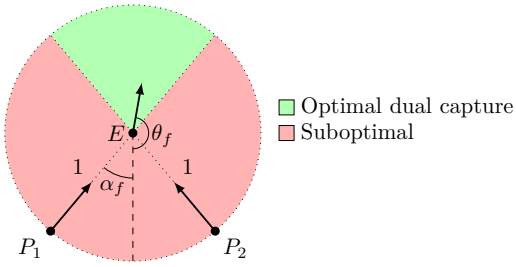

Fig. 2. Optimality of the terminal Evader heading sectors.

Fig. 2 summarizes Proposition 1, showing the sectors of θ_f for optimal dual capture (green), and where dual capture is suboptimal (red).

Lemma 6 (Symmetric dual capture)**.** *For initial conditions with $d_1 = d_2$, the optimal control is $\theta(t) = \pi$, $\forall t \in [0, t_f]$, E's trajectory is straight in the realistic plane, and the scenario terminates in dual capture.*

Proof. Suppose $\left(d_{1_f}, d_{2_f}, \alpha_f\right) = (1, 1, \alpha_f)$ and $\theta_f = \pi$. From Eq. (25) $\kappa = 1$ and so $\lambda_{d_{1_f}} = \lambda_{d_{2_f}}$. Substituting into Eq. (13) with $\lambda_{\alpha_f} = 0$ (from Eq. (17)) gives $\dot{\lambda}_{\alpha_f} = 0$ which implies that $\dot{\lambda}_{d_1} = \dot{\lambda}_{d_2} = \dot{\lambda}_{\alpha} = 0$. So $\lambda_{d_1} = \lambda_{d_2}$, $\forall t \in [0, t_f]$. From Eqs. (20)–(23), then, $\theta^*(t) = \pi$, $\forall t \in [0, t_f]$. Also, Eq. (5) implies $d_1(t) = d_2(t)$, $\forall t \in [0, t_f]$ as a result of this control. Thus any point that starts with $d_1 = d_2$ can be reached (retrogressively) from such a trajectory. The global Evader heading $\Theta = \beta + \alpha + \theta$ thus becomes $\Theta = \beta + \alpha + \pi$. Its time rate of change is $\dot{\Theta} = \dot{\beta} + \dot{\alpha}$, which, from Eq. (5), gives $\dot{\Theta} = 0$ since $d_1 = d_2$ and $\theta = \pi$ along the trajectory. □

Suppose the initial state is s.t. dual capture is optimal. If $d_1 = d_2$, then Lemma 6 applies and the Evader's optimal control is $\theta^*(t) = \pi$. In the general case where $d_1 \neq d_2$, however, the optimal control can only be obtained by solving the TPBVP:

$$\theta_f^*,\ \alpha_f^*,\ t_f^* = \underset{\theta_f,\alpha_f,t_f}{\arg\min} \left\| \begin{matrix} d_{1_0} - d_1(0;\theta_f,\alpha_f,t_f) \\ d_{2_0} - d_2(0;\theta_f,\alpha_f,t_f) \\ \alpha_0 - \alpha(0;\theta_f,\alpha_f,t_f) \end{matrix} \right\|, \tag{28}$$

where $\theta_f \in [\pi-\alpha_f, \pi+\alpha_f]$ and $(d_{1_0}, d_{2_0}, \alpha_0)$ are obtained using Eq. (1), based on the initial Cartesian coordinates of the three agents. Given θ_f, the terminal adjoint values are

obtained by Eqs. (25)–(27). The quantities $\mathbf{x}(0;\theta_f,\alpha_f,t_f)$ are obtained by integrating Eqs. (5) and (10)–(13) backwards from t_f to 0. The trajectory obtained is then converted to the global coordinates via Eq. (1) and then shifted and rotated to match the original global configuration. This process is repeated in a backwards shooting numerical solution scheme – `NLopt` is used with the COBYLA (Constrained Optimization by Linear Approximation) solver to solve Eq. (28) based on an initial guess [17], [18]. With the solution to Eq. (28) in hand, the Evader may compute $\theta(t)$, the optimal control along every point in the trajectory, from Eq. (23).

C. Full Solution

Based on the solution characteristics established above, the state space $\mathscr{C} \equiv \{(d_1,d_2,\alpha) \mid d_1,d_2 \geq 1 \text{ and } 0<\alpha<\frac{\pi}{2}\}$ is partitioned into three regions corresponding to the different terminal scenarios:

$$\mathscr{C} = \cup \begin{cases} \mathcal{R}_1, & \{(d_1,d_2,\alpha) \mid d_{1_f}=1, d_{2_f}>1\} \\ \mathcal{R}_2, & \{(d_1,d_2,\alpha) \mid d_{1_f}>1, d_{2_f}=1\} \\ \mathcal{R}_{1,2}, & \{(d_1,d_2,\alpha) \mid d_{1_f}=1, d_{2_f}=1\} \end{cases}, \quad (29)$$

with the following control modes

$$\theta^*(t) = \begin{cases} \pi-\alpha(t), & (d_1,d_2,\alpha)\in\mathcal{R}_1 \\ \pi+\alpha(t), & (d_1,d_2,\alpha)\in\mathcal{R}_2 \\ \text{solution to TPBVP}, & (d_1,d_2,\alpha)\in\mathcal{R}_{1,2} \end{cases}. \quad (30)$$

Fig. 3 depicts this partitioning of $\mathscr{C}$. The green trajectories correspond to dual capture trajectories with $\theta_f=\pi-\alpha_f$ and the red trajectories correspond to dual capture trajectories with $\theta_f=\pi+\alpha_f$, across the range of α_f. All of the trajectories terminate on the line $\{(d_{1_f},d_{2_f},\alpha_f) \mid d_{1_f}=d_{2_f}=1\}$. Given a particular initial condition, the information in Fig. 3 is enough to determine the corresponding terminal scenario. Note the two separating surfaces form a boat-hull shape in which the black line forms the bottom and the trajectories along $\alpha=0$ form the front. A more human-readable representation is given in Fig. 4 wherein the initial Pursuer positions are fixed and the Evader's initial position is varied over the realistic plane. The numbered blue points in Fig. 4 correspond to initial Evader positions for each of the example simulations contained in the following section.

In lieu of storing some representation of the regions or their partitioning surfaces to determine the optimal capture scenario, Algorithm 1 contains a procedure for computing the optimal control.

V. Simulations

In this section, four simulations are carried out, demonstrating the solution characteristics described in the previous section. Fig. 4 shows the Evader initial positions for each of the simulations. The Pursuers' initial positions are $(\pm 10, 0)$ for all of the examples. Note that Figs. 3 and 4 are shown for a speed ratio of $\mu=0.8$. All of the simulations contained herein are based on the same speed ratio. Table I summarizes the simulation parameters and identifies the unique feature of each example.

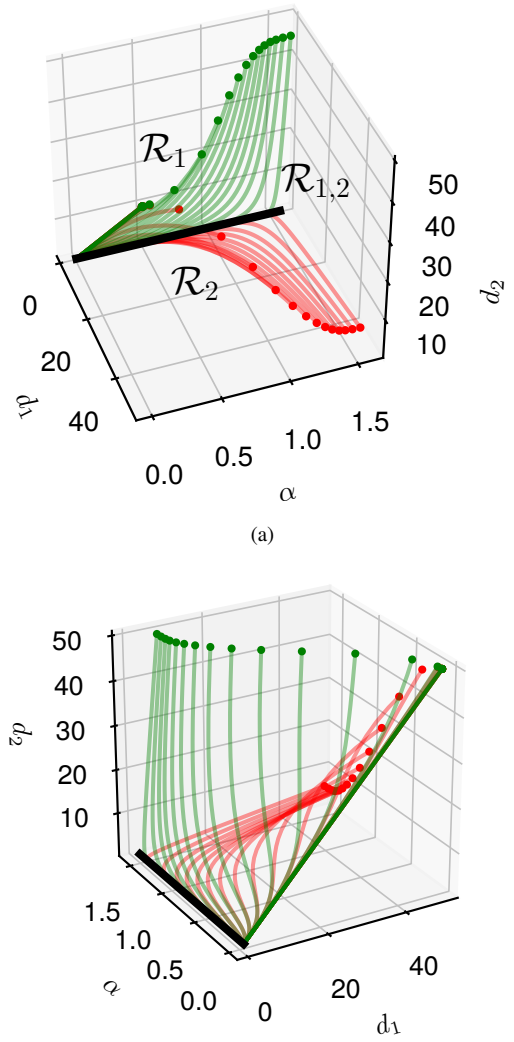

(a)

(b) Rotated view of (a)

Fig. 3. A partitioning of the state space into regions associated with each type of capture.

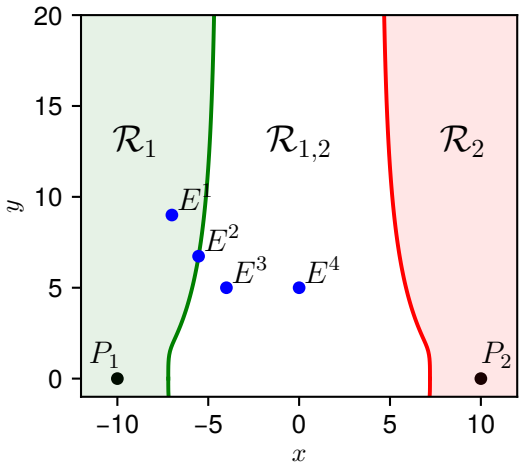

Fig. 4. A representation of the partitioning of $\mathscr{C}$ in the realistic plane for given Pursuer initial positions for various Evader initial positions.

Algorithm 1 Optimal Evasion Against Dual Pure Pursuit

Require: $(d_{1_0}, d_{2_0}, \alpha_0)$

if $d_1 = d_2$ **then**
  $\theta(t) \leftarrow \pi$
else
  $i \leftarrow \arg\min_{1,2} \overline{PE}$
  Forward shoot assuming E flees from P_i until capture
  if P_i captures **then**
    $\theta(t) \leftarrow \pi \mp \alpha(t)$ ▷ depending on $i = 1$ or 2
  else
    $\theta(t) \leftarrow$ solution of TPBVP ▷ Eq. (28)
  end if
end if

TABLE I
EXAMPLE SIMULATIONS PARAMETERS AND DESCRIPTION

#	x	y	Description
1	-7	9	Solo capture by P_1
2	-5.53	6.73	Limiting solo/dual capture
3	-4	5	General dual capture
4	0	5	Symmetric dual capture

For the first example, the Evader's initial position is s.t. the system state is in $\mathcal{R}_1$ and thus the scenario ends in solo capture by P_1. As proven in Lemma 2, the trajectories (in the realistic plane) are straight for E and P_1. Fig. 5 shows the trajectories for this example.

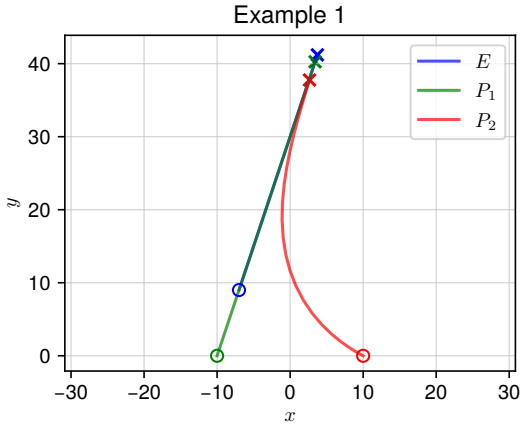

Fig. 5. Example 1: Solo capture by P_1.

In the second example, the Evader's initial position is s.t. the system state lies on the border between $\mathcal{R}_1$ and $\mathcal{R}_{1,2}$. This is the limiting case of solo/dual capture wherein the Pursuer who is initially further away terminates at exactly the capture distance, but the trajectories for P_1 and E are straight (as in solo capture). Lemma 5 proves this behavior. Fig. 6 shows the trajectories for this example.

In the third example, the Evader's initial position is s.t. the system state lies in $\mathcal{R}_{1,2}$, thus the scenario terminates with both Pursuers capturing the Evader simultaneously. These trajectories were obtained via backwards shooting to the specified initial conditions (c.f. Table I). Fig. 7 shows the trajectories obtained for this example.

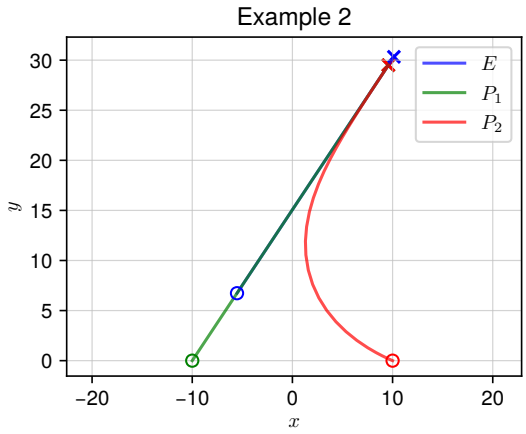

Fig. 6. Example 2: Limiting solo/dual capture.

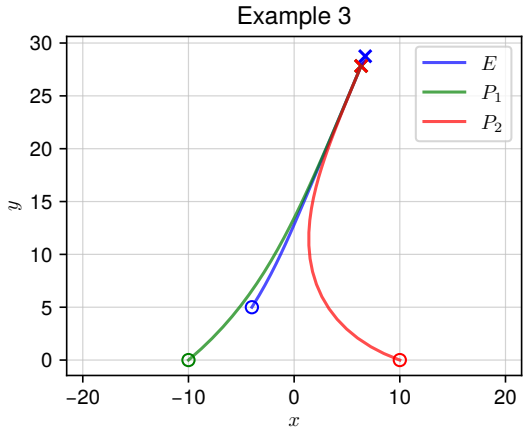

Fig. 7. Example 3: General dual capture.

In the fourth example, the Evader's initial position is equidistant to the two Pursuers, thus satisfying the conditions of Lemma 6. The resulting Evader trajectory is straight in the realistic plane and the Pursuers' trajectories are symmetric. Fig. 8 shows the trajectories for this example.

VI. CONCLUSION

In this paper we solved the optimal control problem of pursuit-evasion type wherein an Evader seeks to maximize its life in the presence of two faster Pursuers using Pure Pursuit who have a finite capture radius. The optimal control was obtained via Pontryagin's Minimum Principle and the complete state space was filled with optimal trajectories. Optimal trajectories terminating in an isochronous (dual) capture by both Pursuers produce a singularity which was rectified by analyzing the limiting Evader heading. A partitioning of the state space was generated based off of the solution characteristics separating into regions of capture by P_1 alone, by P_2 alone, and by both simultaneously. In the dual capture case, a two-point boundary value problem was posed and a procedure, based on backwards shooting, was described. Alternatively, for onboard implementation in a feedback control sense, since the entire state space was

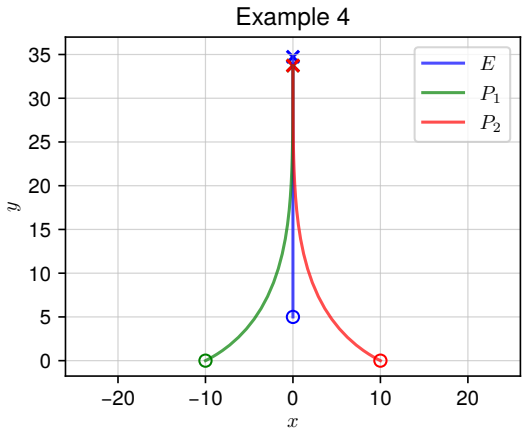

Fig. 8. Example 4: Symmetric dual capture.

filled with optimal trajectories, one may sample the state space to generate a lookup table for the Evader's instantaneous heading. There are two likely research directions for furthering and utilizing these results: (1) comparison (and simulation) against the optimal game policies, wherein the Pursuers seek to minimize the Evader's life, and (2) using the Value function from this problem to make task assignments in larger scenarios involving many agents.

Acknowledgment

This paper is based on work performed at the Air Force Research Laboratory (AFRL) *Control Science Center of Excellence*. Distribution Unlimited. 27 Aug 2019. Case #88ABW-2019-4181.

References

[1] R. Isaacs, *Differential Games: A Mathematical Theory with Applications to Optimization, Control and Warfare*. Wiley, New York, 1965.

[2] E. Garcia, Z. E. Fuchs, D. Milutinović, D. W. Casbeer, and M. Pachter, "A geometric approach for the cooperative two-pursuer one-evader differential game," *IFAC-PapersOnLine*, vol. 50, pp. 15209–15214, 2017.

[3] M. Pachter, "Isaacs' two-on-one pursuit evasion game," in *18th International Symposium on Dynamic Games and Applications (ISDG)*, 2018.

[4] M. Pachter, A. Von Moll, E. Garcia, D. Casbeer, and D. Milutinović, "Two-on-one pursuit," *Journal of Guidance, Control, and Dynamics*, vol. 42, no. 7, 2019.

[5] M. Pachter, A. Von Moll, E. Garcia, D. Casbeer, and D. Milutinović, "Singular trajectories in the two pursuer one evader differential game," in *2019 International Conference on Unmanned Aircraft Systems*, 2019.

[6] Z. E. Fuchs, E. Garcia, and D. W. Casbeer, "Two-pursuer, one-evader pursuit evasion differential game," in *2018 IEEE National Aerospace and Electronics Conference (NAECON)*, pp. 456–464, IEEE, 2018.

[7] M. Pachter and P. Wasz, "On a two cutters and fugitive ship differential game," *IEEE Control Systems Letters*, vol. 3, pp. 913–917, 10 2019.

[8] R. Anderson, "Defender-assisted evasion and pursuit maneuvers," Master's thesis, Air Force Institute of Technology, 2018.

[9] E. Garcia, D. Casbeer, K. D. Pham, and M. Pachter, "Cooperative aircraft defense from an attacking missile using proportional navigation," in *AIAA Guidance, Navigation, and Control Conference*, AIAA SciTech Forum, American Institute of Aeronautics and Astronautics, 2015.

[10] I. Weintraub, E. Garcia, D. Casbeer, and M. Pachter, "An optimal aircraft defense strategy for the active target defense scenario," in *AIAA Guidance, Navigation, and Control Conference*, American Institute of Aeronautics and Astronautics, 1 2017.

[11] V. R. Makkapati, W. Sun, and P. Tsiotras, "Optimal evading strategies for two-pursuer/one-evader problems," *Journal of Guidance, Control, and Dynamics*, vol. 41, pp. 851–862, 2018.

[12] D. Leone, "That time north korea fired sa-2 sams at sr-71 blackbird." NEWS article, 2018.

[13] A. Von Moll, D. Casbeer, E. Garcia, D. Milutinović, and M. Pachter, "The multi-pursuer single-evader game: A geometric approach," *Journal of Intelligent and Robotic Systems*, vol. 96, pp. 193–207, 2019.

[14] A. Von Moll, M. Pachter, E. Garcia, D. Casbeer, and D. Milutinović, "Robust policies for a multiple pursuer single evader differential game," *Dynamic Games and Applications*, pp. 202–221, 2019.

[15] V. R. Makkapati and P. Tsiotras, "Optimal evading strategies and task allocation in multi-player pursuitevasion problems," *Dynamic Games and Applications*, 2019.

[16] D. Li, J. B. Cruz, G. Chen, C. Kwan, and M.-H. Chang, "A hierarchical approach to multi-player pursuit-evasion differential games," in *Proceedings of the 44th IEEE Conference on Decision and Control*, pp. 5674–5679, 2005.

[17] S. G. Johnson, "The nlopt nonlinear-optimazation package," 2019. Accessed 2019-8-01.

[18] M. J. D. Powell, *A Direct Search Optimization Method That Models the Objective and Constraint Functions by Linear Interpolation*, pp. 51–67. Springer Netherlands, 1994.